The Egyptian Journal of Hospital Medicine (July 2019) Vol. 76 (1), Page 3380-3391

Role of Diffusion-Weighted MRI in Hepatocellular Carcinoma Patients Following Transarterial Chemoembolization (TACE)

Mohammed Taha Abd El Hak[1], Nadia Abd El Sater Metwally [1], Ahmed Sobhy Mohammed Abdrabo [2].
Radiodiagnosis, Faculty of Medicine (for Girls, Cairo), Al-Azhar University [1],
Radiodiagnosis, Al-Azhar University (El Bank El Ahli Hospital) [2].
Corresponding author: **Ahmed Sobhy Mohammed Abdrabo ,email:**dr.ahmedsobhy@hotmail.com [3]

ABSTRACT

Background: Hepatocellular carcinoma is one of the commonest cancers all over the world with very high mortality rates. TACE is used to deliver chemotherapeutic agents locally to the tumor.

Aim of the work: The purpose of this study was to evaluate the role of diffusion-weighted MRI and ADC value in comparison with dynamic MRI in the assessment of response and necrosis to treatment of hepatocellular carcinoma after transcatheter arterial chemoembolization.

Patients and Methods: Precontrast T1, T2, STIR, respiratory triggered diffusion-weighted (b factor 20, 500 and 800 s/mm2) and dynamic contrast enhanced MR images obtained in 50 patients with HCC who underwent TACE. Diffusion-weighted MR images, gadolinium-enhanced MR images after TACE were assigned confidence levels for postoperative HCC recurrence.

Results: Dynamic MRI had a sensitivity of 90.5%, a specificity of 96.6%, a positive predictive value of 95 %, a negative predictive value of 93.3% and overall agreement of 94%. Compared to 95.83%, 69.23%, 74.19%, of 94.74% and 82% respectively of diffusion-weighted imaging. The difference between the malignant and negative groups' ADC variables were statistically significant (P value 0.006). The ROC curve showed that the area under the curve is C = 0.728 with SE = 0.075 and 95% CI from 0.582 to 0.874.

Conclusion: Diffusion-weighted MR imaging has lower specificity compared to dynamic MRI with increased false positives. We suggest that the increase is due to intra-lesional hemorrhage or liquefactive necrosis causing diffusion restriction. Diffusion-weighted imaging may act as a supplementary sequence to compensate the dynamic MRI in patients who could not hold their breath adequately.

Keyword: HCC - Post TACE - DWI - Locoregional treatment - Liver.

INTRODUCTION

HCC is a frequent and aggressive malignant tumor, estimated to range sixth by incidence and second by mortality in the global cancer statistics. The high ratio of mortality to incidence (0.95) and the close geographic correlation between incidence and mortality reflects the dismal prognosis. However, longer survival can be reached in early diagnosed and properly treated cases. Liver cirrhosis of any aetiology represents the single largest risk factor of HCC and is found in 70–90% of cases. Worldwide, hepatitis B virus (HBV) infection accounts for more than 50% of HCC cases. In comparison to non-infected individuals, the relative risk of HCC is increased 100-fold in HBV-infected persons, and the risk further increases if HBV-infected patient develops cirrhosis, has longer duration of infection and higher virus burden in blood. The yearly risk of HCC in HBV-infected patients is 2%, although nowadays an increasing proportion of HCCs develops in non-fibrotic liver or on the background of mild fibrosis [(1).]

In the past few years with significant advances in surgical treatments and locoregional therapies, the short-term survival of HCC has improved but the recurrent disease remains a big problem. The pathogenesis of HCC is a multistep and complex process, wherein angiogenesis plays an important role [(2)].

Generally, surgical resection is the gold standard therapy for HCC, unfortunately; only 10–15% of HCC patients are eligible for liver resection due to the severity of underlying cirrhosis or the diffuse distribution of the tumor. Another treatment option is liver transplantation which is theoretically the best treatment for HCC. Currently, ablative therapies are alternative choice for patients with liver tumors who are not eligible for surgery. These therapies are known to have low morbidity and mortality, as well as being less expensive than surgical resection with the ability to perform these procedures on outpatients [(3)].

TACE, using iodized oil mixed with anticancer agents, has been widely used. Iodized oil is used as a vehicle to transport the anticancer drug, and the embolic material enhances the effect of the anticancer drug [(4)].

TACE affects the tumor to the maximum impact of chemotherapy by selective or super-selective injection of supplying tumor vessels by chemotherapeutic agents and decreasing the tumoral blood supply by the embolization of particles leading to prolongation of the contact between the chemotherapeutic agents and HCC [(3)].

Besides, detecting and diagnosing the lesions, contrast enhanced computed tomography (CT) and magnetic resonance imaging (MRI) are widely used in

Received:6/4/2019
Accepted:5/5/2019

the post-treatment follow-up of these patients, for the detection of residual or recurrent tumors after treatment, as well as for the depiction of post-treatment complications. There is suggestive evidence that MRI is more accurate than other radiological modalities in the detection of residual or recurrent tumors [(3)].

Monitoring the effectiveness of transarterial chemoembolization (TACE) with imaging is important in determining treatment success and in guiding future therapy. However, imaging techniques and imaging response criteria have been limited in giving clinically satisfactory information about the extent of tumor necrosis [(5)].

Unenhanced CT confirms successful introduction of the chemoembolization mixture into the targeted lesions. However, it can be difficult to evaluate contrast enhancement in a tumor with partial retention of iodized oil on contrast- enhanced CT because of the beam hardening artifacts produced by the high attenuation of iodized oil. The signal intensity of MRI is not degraded by the presence of iodized oil; therefore, a residual viable tumor is better defined by MRI [(6)].

Magnetic resonance (MR) imaging of the liver is an important tool for the detection and characterization of focal liver lesions and for assessment of diffuse liver disease, having several intrinsic characteristics, represented by high soft tissue contrast, avoidance of ionizing radiation or iodinated contrast media. More recently, the detection and characterization of focal liver lesions is assessed by application of several functional imaging techniques (i.e., diffusion-weighted sequences, hepatobiliary contrast agents, perfusion imaging, magnetic resonance (MR)-elastography and radiomics analysis – in which multiple molecular and other biomarkers are used in for prediction of treatment response-). MR functional imaging techniques are extensively used both in routine practice and in the field of clinical and pre-clinical research because, through a qualitative rather than quantitative approach, they can offer valuable information about tumor tissue and tissue architecture, cellular biomarkers related to the hepatocellular functions [(6)].

Diffusion weighted (DW) MR imaging is used to measure difference in microstructures that are based on the random displacement of the water molecules these differences in water mobility are quantified by apparent diffusion coefficients (ADCs). The ADC reflects the signal loss on DW images that occurs with increasing *b* value and is inversely correlated with tissue cellularity [(7)].

Diffusion weighted imaging (DWI) in the liver is a relatively new and increasingly used imaging technique in addition to conventional unenhanced and contrast enhanced MRI. DWI proved to be helpful in the characterization of focal liver lesions, but should always be used in conjunction with traditional MRI. DWI in the follow-up after TACE shows promising results in the detection of ablation site recurrences, especially in combination with conventional contrast enhanced imaging [(8)].

AIM OF THE WORK

The aim of this study was to evaluate the role of MRI Diffusion with ADC mapping in the detection of recurrent or residual tumor viability after transarterial chemoembolization procedure and the possible complications that may be encountered during the procedure. It was aimed by the study to improve the DWI technique used after interventional therapy for malignant hepatic tumors.

PATIENTS AND METHODS

Patients:

This prospective study was performed on 50 cases of HCC who underwent TACE.

The study was conducted in Bab EL Shariea University Hospital. The patients were referred from the Tropical Department to the Radiology Department over a period of 24 months (June 2016–June 2018). The patients' age ranged from (40 to 79) years old (mean age, 59.6 ± 11.2); 40 patients were males and 10 were females. All patients had liver cirrhosis related to chronic viral hepatitis.

Approval of Al-Azhar Ethical Committee and informed consent from each patient were obtained.

Inclusion Criteria:

Patient with hepatocellular carcinoma suitable for TACE.

Exclusion criteria:

1-Contraindications to contrast media, e.g. patients with renal failure and patients allergic to contrast media.

2-Patient who has one or more of relative or absolute MRI contraindication.

3-Other tumors rather than hepatocellular carcinoma

All cases had been subjected to the following:

Pre-imaging:

• Full clinical assessment including (age, sex and clinical presentation)

• Revision of the patient's laboratory investigations including (renal function tests, blood urea, serum creatinine and coagulation profile).

• Revision of the radiological investigations previously done for the patients (US, CT, MRI, …).

• All patients were scheduled to undergo dynamic MRI with DWI within 90 days after one or more treatments of TACE. In case of absent evidence of residual, follow up was done within 90 days after the first MRI.

• MRI was performed using 1.5-T MRI scanner (Philips Medical system, Intera, Netherland) equipped with phased-array torso surface coil with patient in supine position, immobilized and in a comfortable position.
• Fasting 4-6 hours before examination was needed in all 50 patients.
• Sedation was needed in 2 patients and no anthesis was needed for any patient.

Imaging:

1. **Precontrast conventional protocol includes:**
- Axial T1WIs (TR = 10msec, TE = 4.6msec, flip angle = 15°).
- Axial T2 WIs (TR = 560msec, TE = 26-28msec, flip angle = 90°).
- Axial T2 fat suppression (SPAIR) (TR = 560msec, TE = 26-28msec, flip angle = 90°).
- We used FOV = 315–350 mm, slice thickness = 7 mm, interval = 2 mm for all axial precontrast sequences.
- Coronal T1 WIs.
- Coronal T2 WIs.

2. **DWIs Protocol used**
- Performed before the dynamic study using respiratory triggering fat-suppressed single shot spin echo-planar sequence.
- Obtained by applying b values of (20, 500 and 800 s/mm2).
- Parallel imaging with generalized auto- calibrating partially parallel acquisition (GRAPPA) with an acceleration factor of two was applied to reduce the acquisition time. The other parameters were as follows: repetition time (TR) ≥1890 msec, echo time (TE) = 70 msec, number of excitations (NEX)=3, matrix 124 x 120 with a field of view as small as possible, slice thickness 7-8mm, slice gap 1-2 mm and scan time 4-5 min.

3. **Dynamic contrast enhanced protocol**
- Done after diffusion study to avoid the effect of contrast agents on ADC value.
- Performed after bolus injection of 0.1 mmol/kg body weight of Gd-DTPA, flushed with 20 ml of sterile saline solution from the antecubital vein. The injection of contrast and saline was performed manually.
- Performed using 3D fat-suppressed T1-weighted gradient echo (THRIVE) sequence. Dynamic series consisted of one pre contrast series and then three successive post contrast series including early arterial, late arterial and portal phases with 19–21 s intervals. This was followed by delayed phase imaging at 5-min. Patients were examined in end expiration to limit the possibility of image misregistration.
- Acquisition parameters were flip angle = 10; matrix size = 172x135; field of view = 300–400 mm and slice thickness = 2–3 mm.

4. **ADC map**
- ADC map and ADC value: ADC maps were generated on the workstation. The three b values (50, 500 and 800 sec/mm2) were used for ADC calculation.
- Calculation of the ADC value was an automated process available on the workstation.

MR images were analyzed for the following:
- The morphological features of each lesion included (size, border, signal characteristics at T1, T2 and FAT SATURATED signal characteristics).
- Pattern of enhancement in the (dynamic imaging, subtracted images and color mapping).
- Signal intensity on diffusion images with ADC values.
- ADC measurement:
  ADC was calculated with linear regression analysis of the function S = S0 × exp (–b × ADC), where S is the signal intensity after application of the diffusion gradient and S0 is the signal intensity at a b value of 0 s/mm2. The three b values (20, 500 and 800 s/mm2) were used for ADC calculation
- For precise placement of circular ROI in the small lesions, the center of the lesion on the DWI was determined by the interfacing point of two lines met at right angle, which are perpendicular line and a horizontal line from the upper and the left border of the images, respectively. With the knowledge of the length of each line, the identical lines could be drawn on the corresponding ADC map. With the reference of the lesion size on DWI, circular ROI was placed around the center point to measure the ADC of the lesion.
- A region of interest was drawn over any sustaining hyperintensity areas on diffusion images and if no high signal can be identified, the whole lesion was measured. The ADC was measured three times and the three measurements were averaged.

Statistical Analysis
- Computer software package SPSS version 15 was used in the analysis.
- For quantitative variables, mean (as a measure of central tendency), standard deviation (as measures of variability) were presented.
- Frequency and percentages were presented for qualitative variables.
- Chi-Square test was used to estimate differences in qualitative variables.
- A ROC (Receiver Operating Characteristic) curve was constructed and the area below the ROC curve was used to represent prediction precision.

- P-values less than 0.05 were considered as statistically significant.

RESULTS

This prospective study was conducted on 50 patients and the results were analyzed as follows:

1. Demographic Data

- The patients' age ranged between 40 to 79 years old (mean age 59.6 ± 11.2) years.

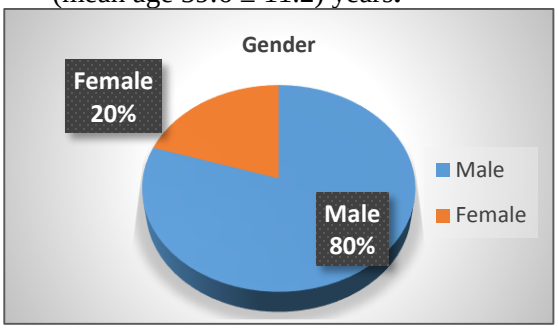

Figure (1): Distribution of patients according to gender

- Child Pugh's Score: -

Forty-eight patients (96%) had Score A. Two patients (4%) had Score B. No patient with score C.

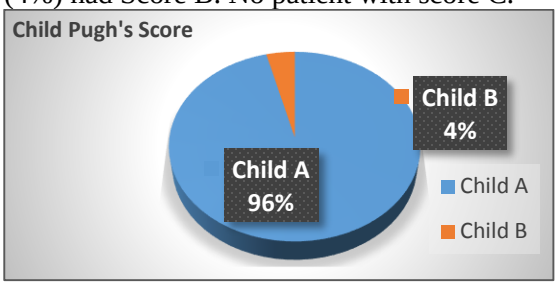

Figure (2): Distribution of patients according to their Child Pugh's Score.

- Ascites:

Among the 50 patients, forty-one (82%) patients had no ascites, eight (16%) with mild ascites and one (2%) had moderate ascites.

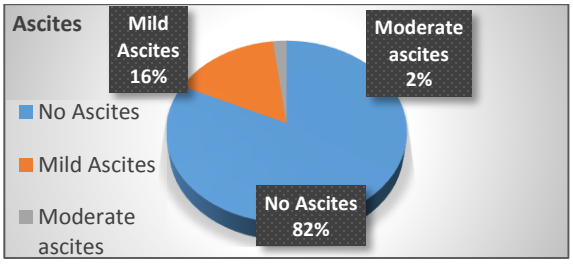

Figure (3): Distribution of patients according to presence of ascites

2. Final Diagnosis

It was difficult to obtain pathologic confirmation in patients who underwent chemoembolization because most of them did not undergo surgery. In addition, biopsy could have resulted in sampling error. So, the standard of reference was: -

- Residual/recurrent HCC finally diagnosed depending on the follow-up image findings of further tumor growth or sustained iodized-oil accumulations in the hyper vascular area on the hepatic arteriography with repeated TACE.
- For the negative conditions including the (inflammatory or ischemic changes, or pseudo lesions by abnormal vascular perfusion in the perilesional hepatic parenchyma), the perilesional abnormal signal intensity area should disappear or decrease in size on MRI in 3 months follow up.

The "negative lesions" group included 29 patients (58%), while the "malignant lesion" group included 21 patients (42%).

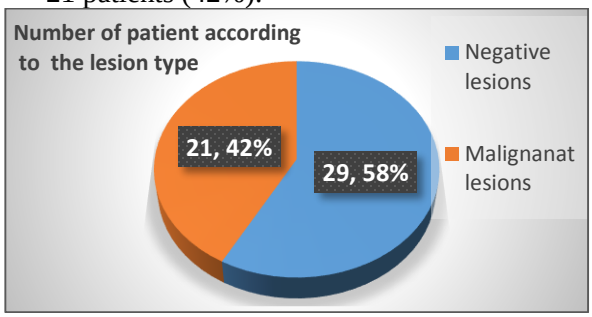

Figure (4): Distribution of lesions into negative and malignant groups.

3. Analysis of lesions characteristics:

- Size:

The size of chemo-embolized lesions ranged from 1.5 to 8.5 cm. the maximum, minimum, mean and standard deviation of both malignant and negative groups are illustrated in (Table 1).

Table (1): represents the minimum and maximum diameter of the lesions in cm.

Dimension	Negative	Residual
Minimum	***1.5***	***1.7***
Maximum	***8.5***	***6***
Mean+/- SD	***3.8 +/- 1.90***	***3.52 +/-1.30***

- Signal Intensity:

The signal intensity of negative conditions on T1 and T2 sequences is illustrated in (Figure 5).

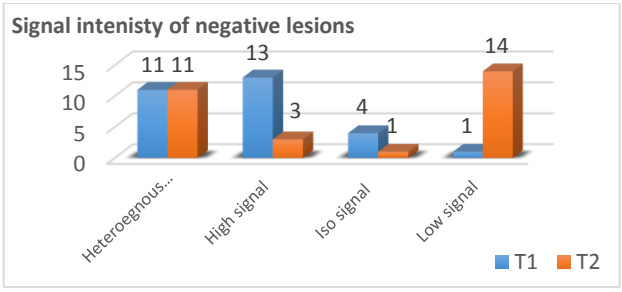

Figure (5): Distribution of signal intensity of negative conditions on T1 WIs and T2 WIs.

The signal intensity of residual lesions on T1 and T2 sequences is illustrated in figures (6).

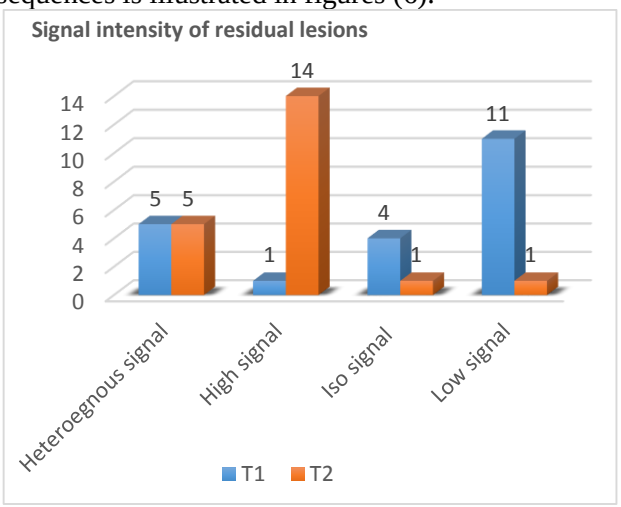

Figure (6): Distribution of signal intensity of residual lesions on T1 WIs and T2 WIs

The border of negative conditions and malignant residuals were classified into smooth, irregular and nodular. 86% of negative conditions were circular compared to 52.3 % of residual lesions (Figure 7).

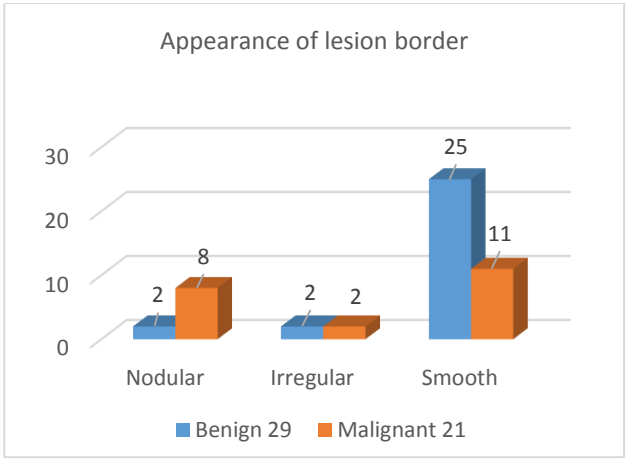

Figure (7): Distribution of lesion border in both negative and malignant conditions.

4. Analysis and interpretation of diagnostic indices of dynamic and diffusion MRI:

- **Dynamic MRI:**

Arterial hypervascularity and subsequent washout were regarded as suggestive findings of viable HCC for the precontrast T1-w hypointense and T2-w hyperintense portions.

Negative conditions were considered when progressive or persistent enhancement was detected on dynamic images.

Correlating the dynamic findings and the final diagnoses, two cases were found to be false negative (4%), one case was false positive (2%), 28 were true negative (56%) and 19 were true positive (38%), as shown in table (2).

Table (2): Correlating dynamic MRI results to the final diagnosis in the studied group.

Dynamic results	Number of lesions	Percentage (%)
FN	2	4 %
FP	1	2 %
TN	28	56 %
TP	19	38 %
Total	50	100 %

Based on the previous findings, dynamic MRI had a sensitivity of 90.5%, a specificity of 96.6%, a positive predictive value of 95 %, a negative predictive value of 93.3% and overall agreement of 94%.

Regarding the false positive case by dynamic MRI, a perilesional early arterial enhancement with wash out on delayed phase becoming isointense to surrounding liver was observed. So, it was considered as a residual tumor. Yet, on repeated angiography no blush was detected. Follow up CT after 3 months was free. Upon reviewing the MRI of the patient, the arterially enhancing area was isointense on delayed phase of dynamic MRI besides no corresponding signal intensity changes were noted on T1, T2 and STIR-weighted images. Findings were in favor of perilesional arterioportal shunt. Diffusion images in this case showed no restriction of diffusion.

Regarding the false negative cases by dynamic MRI, inadequate breath holds by the patient led to motion artifact with subsequent misinterpretation by the viewer.

- **Diffusion MRI**

All DWI images using different b values were sorted for the confidence levels according to three grade scales:

Negative conditions were considered when low signal intensity on diffusion images is noted or mild sustained hyperintensity with bright ADC map (T2 shine through effect) is noted.

Uncertainty is considered when sustained faint or moderate hyperintensity is seen on diffusion images with iso-intensity on ADC maps.

Viable tumor portion was identified by a sustaining hyperintensity in the diffusion images compared with the signal drop of background parenchyma with increasing b factors combined with low ADC map.

Intensity on diffusion images was scaled (mild, moderate or marked) compared to the spinal cord on (*b* value 800).

-When we regarded the confidence level of 2 (uncertainty) as a negative interpretation, we had the following indices: -

Upon correlating the diffusion findings to the final diagnoses, five cases were found to be false negative (10 %), six cases were false positive (12%), twenty-three were true negative (46%) and sixteen were true positive (32%), as shown in table (3).

Table (3): Correlating diffusion MRI results to the final diagnosis in the studied group upon regarding the confidence level of 2 as a negative interpretation.

Diffusion results	**Number of lesions**	**Percentage (%)**
FN	5	10 %
FP	6	12 %
TN	23	46 %
TP	16	32 %
Total	50	100 %

Based on the previous findings, diffusion MRI had a sensitivity of 76.19 %, a specificity of 79.31 %, a positive predictive value of 72.73% and a negative predictive value of 82 .14 % and overall agreement of 78%.

-When we regarded the confidence level of 2 (uncertainty) as a positive interpretation, we had the following indices: -

Upon correlating the diffusion findings to the final diagnoses, one case was found to be false negative (2%), eight cases were false positive (16%), eighteen were true negative (36%) and twenty-three were true positive (46%) as shown in table (4).

Table (4): Correlating diffusion MRI results to the final diagnosis in the studied group upon regarding the confidence level of 2 as a positive interpretation.

Diffusion results	Number of lesions	Percentage (%)
FN	1	2 %
FP	8	16 %
TN	18	36 %
TP	23	46 %
Total	50	100 %

Based on the previous findings, diffusion MRI had a sensitivity of 95.83%, a specificity of 69.23%, a positive predictive value of 74.19%, a negative predictive value of 94.74% and overall agreement of 82%.

If we regarded the confidence levels of 2 as a positive interpretation, the overall sensitivity increased from 76.19 % to 95.83%, while the specificity decreased from 72.4 % to 69.23%.

Therefore, the sensitivity, specificity, PPV, NPV and Overall agreement calculated for both the dynamic imhjkmmkages. For the DWI, they were as shown in table (5).

Table (5): The different indices of the dynamic MRI and the DWI

	DYNAMIC MRI	DWI
Sensitivity	**90.5%**	**95.83%**
Specificity	**96.6 %**	**69.23%**
PPV	**95 %**	**74.19%**
NPV	**93.3%**	**94.74%**
Overall agreement	94%	82%

Therefore, addition of DWI to the conventional MR images improved the sensitivity, but decreased the specificity and PPV as it increased the false positives.

-The pattern of diffusion restriction was classified into:

Heterogeneous, Rim and Focal nodular.

Nineteen patients with low signal intensity on diffusion images or mild sustained hyperintensity with bright ADC map (shine through effect) were excluded, with remaining 31 patients with restricted diffusion.

Among the remaining 31 patients, diffusion had 8 false positive (negative) and 23 true positive (residual) cases with their pattern of diffusion as shown in table (6).

Table (6) : Pattern of diffusion restriction among the negative and malignant group according to the final diagnosis.

Pattern of diffusion restriction	**Negative**	**Malignant**	**Total**
Heterogeneous	5	4	9
Rim restriction	1	1	2
Focal nodular	2	18	20
			31

So, 78.26 % of true positive cases exhibited focal peripheral nodular restriction, meanwhile 62.5% of the false positive cases exhibited heterogenous restriction.

Analysis of the ADC value:

The different ADC values elicited from the corresponding ADC maps were calculated. The

difference between ADC variables among the malignant and negative groups were statistically significant (P value 0.006).

(ROC curve) obtained by plot at different cut off values. The best cut off that maximizes sensitivity and specificity is 1.26. At this ADC value, the sensitivity is 0.95 and specificity is 0.41 (1 – specificity = 0. 59). A statistical software showed that the area under the curve is C = 0.728 with SE = 0.075 and 95% CI from (0.582 to 0.874).

It seemed from the ROC that ADC variable is a fair indicator to differentiate marginal recurrence of HCC from perilesional pseudo- or negative lesions. (Area under the curve: - excellent 0.9-1, good 0.8-0.9, fair .7-0.8, poor 0.6-0.7, fail 0.5-0.6).

DISCUSSION

The sensitivity of MRI can be further improved by diffusion-weighted imaging, based on the assessment of Brownian motion of water molecules and water diffusion within a voxel (a tridimensional pixel). Cell membranes limit the diffusion; therefore, greater cellularity is seen also in malignant tumours resulting in diffusion restriction [(9)].

However, fibrosis also decreases the mobility of water molecules. By different modalities, diffusion-weighted imaging can increase the sensitivity for HCC detection, the liver-to-lesion contrast and the specificity in the differential diagnosis with negative cirrhotic nodules [(10)].

Catheter based therapies such as transcatheter arterial chemoembolization, a technique now widely applied for the treatment of hepatic malignancies, aims to deliver treatment to a target tumour volume by means of a percutaneously placed intra-arterial catheter within an artery that supplies the tumour [(11)].

Standardized criteria for measuring tumour response to treatment, have been established by the response evaluation criteria in solid tumours (RECIST). These guidelines use anatomic imaging with one or two dimensional diameter measurements to define tumour size for all aspects of cancer patient management from diagnosis and staging, to monitoring response to therapy and disease progression. However, these measurements are often inadequate for monitoring the acute effects of minimally invasive therapies that cause little or a slow reduction in tumour size, the effectiveness in locoregional therapies are not properly reflected in the WHO and RECIST guidelines [(12)].

The modified RECIST (mRECIST) criteria were developed by the American Association of Liver Disease for evaluation of HCC specifically, where only the viable portion of the tumour is included as the target lesion [(13)].

Lim *et al.* [(4)] stated that CT is still the widely used imaging method to follow up patients. It is done immediately after the TACE procedure to ensure the retention of lipidol by the tumor and after 1 month for detection of any residual or recurrence. At the same time, successful introduction of the chemoembolization mixture limits the utility of CT for assessing tumor necrosis because the presence of the hyperattenuating iodized oil within the lesions of interest makes assessment of residual tumor enhancement difficult.

While **Afifi *et al.*** [(14)] and **Yu *et al.*** [(15)] demonstrated the value of MRI in assessment of HCC necrosis after TACE to avoid the interference of accumulated iodized oil.

Braga *et al.* [(16)] stated that the treated lesion exhibits increased signal intensity on T1-weighted images and decreased signal intensity on T2-weighted images. Among the 50 patients included in our study, about 32% of lesions showed heterogenous signal intensity and 10% of the negative group lesions exhibited high T2 signal intensity, which is consistent with **Afifi *et al.*** [(14)] who reported that T2 signal characteristic showed no significant changes in seventeen patients out of 20 patients in the study. Three patients however showed difference in the T2 appearance manifested by variable degrees of increased signal.

Therefore, it was difficult to assess the viable tumors of HCC after TACE by conventional spine echo imaging. in our study.

Kamel *et al.* [(17)] demonstrated the value of vascular and cellular biomarkers that could be used to assess treatment response. Changes in these biomarkers occur in vivo within hours or days of exposure to antineoplastic agents and they potentially could be used to assess early tumor response. The molecular changes include contrast enhancement and ADC changes at DW MR imaging.

Lee *et al.* [(20)] stated that, on dynamic contrast-enhanced MRI post-TACE enhancement represents either granulation tissue or residual tumoral tissue admixed with necrotic regions. Differentiation depends on the phase of enhancement. Granulation tissues show delayed uptake, whereas residual tumoral tissue gives early arterial enhancement indicating unsuccessful TACE treatment. This is in agreement with **Yu et al.**[(15)] who stated that negative conditions would show a perilesional rind-like contour and hyperintensity on delayed phase postcontrast images and could be distinguished from a more nodular contour and washout of contrast material on the delayed phase of dynamic imaging in residual lesions.

In the experience of **Kim *et al.*** [(21)], image subtraction was helpful for the evaluation of the therapeutic efficacy of TACE in HCCs as the high iodized oil T1 signal makes the assessment of tumor

enhancement difficult on post-contrast T1-weighted images. To accurately assess tumor enhancement, we also used the image subtraction techniques.

In our study, we had relatively lower sensitivity of dynamic MRI compared to other studies done by **Yu *et al.*** [15] and **Goshima *et al.*** [22], as we had two cases in which inappropriate breath holding led to motion artifact with subsequent false interpretation by the viewer. We also had one false positive case due to misinterpretation of a perilesional arterioportal shunt.

Geschwind *et al.* [23] reported that diffusion-weighted imaging can provide an insight about water composition within a tumor and the degree of tumor viability.

Necrotic tumors have increased water diffusion and increase ADC values due to cell membrane damage, whereas viable tumor cells have restriction of water diffusion and relatively low ADC (**Lee *et al.*)** [20].

In the initial clinical study done by **Kamel *et al.*** [19] on patients with HCC who underwent chemoembolization followed by resection, they found direct correlation between increasing ADC and increasing necrosis within the surgical specimens ($r = 0.95$; $p < 0.05$).

Following this study, other studies done by **Ebeed *et al.*** [24] and **Kamel *et al.*** [18], where they confirmed that individuals with HCC who responded to chemoembolization treatment showed a significant increase in the ADC values after therapy.

Sahin *et al.* [25] observed that an absolute increase in ADC values could differentiate viable/contrast-enhancing ($1.42\pm0.25\times10–3$ mm2/s) and necrotic / non-enhancing ($2.22\pm0.31\times10–3$ mm2/s; $p< 0.001$) tumor areas when compared to contrast enhancement patterns 6–8weeks after TACE.

Kamel *et al.* [17] demonstrated that a significant increase in the ADC values following TACE in patients with HCC could be seen as early as 12–24 h after treatment in patients who were subsequently defined as responders by RECIST criteria.

Practically, it is more important to know whether the procedure was complete or incomplete rather than calculating ADC before and after the procedure. In the study of **Yu *et al.*** [15], ADC was measured to characterize the marginal recurrence of HCC from perilesional pseudo- or negative lesions. The results of this study did not demonstrate statistically significant differences; the ADCs varied widely for the non-tumorous lesions and profoundly overlapped with the viable tumor portion making it impossible to determine any cutoff points.

In a study of **Goshima *et al.*** [22] DW-MRI was not found to be a reliable predictor of local HCC recurrence after TACE as compared to gadolinium- enhanced MR imaging. ADC of malignant and negative lesions has been shown to overlap, both within and between different studies with no established cut-off value.

In our study, the difference between ADC variables between the malignant and negative groups were statistically significant P value 0.006. The best cut off that maximizes sensitivity and specificity is 1.26. At this ADC value, the sensitivity was 0.95 and specificity was 0.41 (1 –specificity = 0. 59). We found from the ROC that ADC variable is a fair indicator to differentiate marginal recurrence of HCC from perilesional pseudo- or negative lesions.

Yu *et al.* [15] study stated that DWI increased the sensitivity for determining perilesional tumor recurrence according to the increased confidence level for the sustaining hyperintensity with increasing b factors. However, the number of false positives increased by adding DWI. Although, the decreased specificity compromised the increased sensitivity gained by adding DWI and there was a decrease in the overall diagnostic accuracy.

In our study, we also found that diffusion MRI increased the sensitivity of local HCC detection on the expense of examination specificity due to increased false positives.

Yu *et al.* [15] stated that the increase in false positive findings originated from perilesional parenchymal insults that showed sustaining hyperintensity on DWI with increasing b factors. They demonstrated that hypercellularity intermingled with a fibrotic component in the inflammatory granulation tissue could restrict water diffusion, resulting in sustaining hyperintensity on DWI.

In our study, 8 false positive cases out of 50 patients were misdiagnosed on diffusion weighted imaging. When we reviewed the corresponding pattern of diffusion restriction, 78.2 % of true positive cases exhibited focal peripheral nodular restriction. Meanwhile 62.5% of the false positive cases exhibited intralesional heterogenous restriction. So, we considered that the increase in false positive findings in our study is likely originating from intralesional hemorrhage or liquefactive necrosis that causes diffusion restriction. In the study of **Batra et al.** [28], sterile liquefactive necrosis and intracavitary microhaemorrhage are accepted to be the cause of hyperintensity in diffusion-weighted MR images of post therapeutic necrosis of malignant lesions. Our results are matching with those of **Ebeed et al.** [24], **Yu *et al.*** [15] and **Goshima *et al.*** [22] who stated that dynamic contrast enhanced MRI to be superior to diffusion weighted MRI in evaluating HCC response to treatment. As dynamic MRI had a sensitivity of 90.5%, a specificity of 96.6%, a positive predictive value of 95 %, a negative predictive value of 93.3% and overall agreement of 94% compared

to 95.83%, 69.23%, 74.19%, 94.74% and 82% respectively of diffusion weighted imaging.

In the previous studies done by **Yu *et al.*** [15] and **Goshima *et al.*** [22], a variety of b values were used.

Jiang *et al.* [29] stated that the signal intensity on diffusion-weighted images is a mixture of diffusion and perfusion. On DWI obtained with a low b-value, perfusion effects usually caused larger signal attenuation than diffusion effects. Also they stated that the image quality diminished greatly with increasing b value especially on b 2000 DWI.

Taouli *et al.* [30] found that ADC values were affected by intravoxel perfusion and were usually overestimated when a low b factor was applied. Thus, they avoided using low b factors in their study on liver. Although high b factors of up to 1000 s/mm^2 were required to determine virtually true ADCs, they used a middle-range b factor of 500 s/mm^2, because liver contours were obscured due to weak signals in the liver when high b factors were used, which hampered radiologist interpretation in the clinical setting.

In our study, we used b values 0, 500 and 800 s/mm^2 to avoid intravoxel perfusion effect which result from low b values (less than 50 s/mm^2) as well as image degradation from high b values (more than 1000 s/mm^2).

Chiu *et al.* [31] considered that intravenous contrast agent could affect DWI in two ways. The ADC may decrease slightly because the contrast agent decreases the intravascular signal intensity. This might lead to suppression of the perfusion effect on the calculated ADC. Second, the T2 shortening effect of contrast agent may decrease the signal intensity of the DWI images at b = 0 and b = 500 s/mm^2. In their study, 20 patients were examined and the ADC values were compared before and after administration of contrast agent. They concluded that the ADC values tended to decrease for each focal hepatic lesion and the liver tissue after administration of contrast agent, although they did not reach statistical significance.

In our study as well as in the studies of **Yu *et al*.** [15] and **Goshima *et al.*** [22], DWI was performed before the dynamic imaging to avoid the effect of contrast agents on ADC values.

Koh and Collins [26] stated that breath-hold imaging allows a target volume (e.g. liver) to be rapidly assessed. The images retain good anatomic details and are usually not degraded by respiratory motion or volume averaging. Small lesions may be better perceived and the quantification of ADC is theoretically more accurate than with a non-breath-hold technique. The image acquisition time at each breath-hold is 20–30 s and imaging is typically completed in a few breath-holds. The disadvantages of breath-hold imaging include a limited number of b-value images that can be acquired over the duration of a breath-hold, poorer signal-to-noise ratio compared with multiple averaging methods, and greater sensitivity to pulsatile and susceptibility artefacts.

As advocated by **Kandpal *et al.*** [27] we adopted the use of respiratory-triggered DW to increase the signal-to-noise and contrast- to-noise ratios without compromising the ADC calculations. It requires a 4- to 8-minute acquisition time.

Lin *et al.* [32] stated that on a high b-value DW-MR image, the background may be significantly suppressed, making it difficult to assess areas of restricted diffusion in relation to the anatomical features. Thus they reported that fusion images may be beneficial to combine the unique functional information of DW-MRI or ADC map with the anatomical details provided by the morphologic T1- or T2-weighted sequences.

In our study, application of fusion images for our cases were of little value as respiratory-triggered DW provides us with images of good signal-to-noise and contrast- to-noise ratios.

According to **Ebeed *et al.*** [24] and **Thoeny *et al.*** [33] diffusion weighted MRI has some advantages compared to dynamic MRI. First, contrast medium administration is not required, and the examination is obtained in a relatively short time. Second, the technique is easy to be repeated, allowing close follow-up during and after tumor treatment. Also, image post-processing is less time-consuming compared to dynamic contrast-enhanced MR imaging. At last, diffusion-weighted MR imaging allows easy evaluation of the whole tumor especially being beneficial in cases of inhomogenity that may occur within tumors.

In our study, we also found that respiratory triggered diffusion weighted images compensated the false results by the dynamic MRI in our patients who could not hold their breath adequately.

In our study, we had some diagnostic limitations. First, it was difficult to obtain pathologic confirmation in patients who underwent chemoembolization because all of these patients were not subjected to surgery. Second, lesions included in our study were larger than 1 cm in diameter, and few lesions were located at the hepatic dome. The for mentioned factors could cause selection bias leading to increased sensitivity of diffusion-weighted images since hepatic lesions close to the diaphragm pose a challenge to DW-MRI evaluation as they are more sensitive to motion and susceptibility artifacts.

In conclusion, diffusion-weighted MR imaging has lower specificity compared to dynamic MRI with increased false positives. We suggest that the increase is due to intralesional hemorrhage or liquefactive necrosis causing diffusion restriction. However, diffusion weighted imaging may act as a supplementary

sequence to compensate the dynamic MRI in patients who could not hold their breath adequately.

CONCUSION

Due to the aggressive characteristics and high mortality of hepatocellular carcinoma, as transcatheter arterial chemoembolization has been generally performed in the worldwide institutions for the curative or palliative treatment of this tumor surgical intervention has been decreased.

That's why after TACE, accurate diagnosis of a residual or locally recurrent tumor is crucial. Accurate post TACE diagnosis can facilitate successful management at an early stage of the disease and to avoid complicated or advanced disease that has an unfavorable prognosis.

On one hand, Multiphase dynamic CT is widely used for evaluating the therapeutic effect of TACE according to the degree of uptake and the distribution of the iodized oil within the tumor and the surrounding hepatic parenchyma. It can provide useful information regarding the degree of tumor necrosis. However, a diagnostic dilemma due to defective accumulation of lipiodol either due to necrotic areas or residual tumor still facing radiologists. Also, the hyper-attenuating retained lipiodol causes hardening artifact, which degrades the interpretation of the images.

On the other hand, MRI allows the detection of anatomic, functional and molecular parameters of the tumor as well as the surrounding liver parenchyma in order to assess the response to treatment. Non-contrast T1- and T2-weighted images provide information concerning the morphological changes as well as changes in the fluid content and fibrosis.

In our study, we found that T2 hyperintensity not only represents residual tumor but also could represent hemorrhage, liquefactive necrosis, or inflammatory infiltrate. Here, it was difficult to assess the viable HCC tumors after TACE by conventional spin echo imaging.

Contrast-enhanced MRI is sensitive to therapy-related changes in blood volume and vascular permeability of the lesion, which may be associated with tumor angiogenesis.

Diffusion-weighted image provides an insight about water composition within a tumor to assess the degree of tumor viability. The viable tumor cells have intact membranes that cause restricted water diffusion whereas necrotic tumors have increased water diffusion due to cell membrane disruption.

The apparent diffusion coefficient (ADC) calculated in diffusion-weighted MRI has become a good aiding biomarker of tumor response to therapy. Since it measures the mobility of water within tissues. The viable tumors are highly cellular, and the cells have an intact cell membrane that restricts the mobility of water molecules resulting in a relatively low ADC. Conversely, the cellular necrosis increases membrane permeability, allowing free mobility of water molecules and causing an increase in ADC.

In our prospective study, we evaluated the role played by MRI in the assessment of post chemoembolization of HCC. Fifty patients were evaluated by precontrast T1, T2, fat saturated as well as dynamic contrast-enhanced and respiratory-triggered diffusion-weighted MR sequences. The results were studied and intercorrelated.

The results of this study showed superior diagnostic performance of dynamic MRI compared to diffusion studies as dynamic MRI had a sensitivity of 90.5%, a specificity of 96.6%, PPV of 95 %, NPV of 93.3% and overall agreement of 94% compared to 100%, 65.5%, 67.7%, 100% and 80% respectively of diffusion-weighted imaging.

The diffusion MRI was found to increase the sensitivity of local HCC detection, but on the expenses of examination specificity due to increased false positives. Those false positives may be attributed to the intralesional hemorrhage or liquefactive necrosis that causes diffusion restriction.

In our study, ADC variable was found to be a fair indicator to differentiate marginal recurrence of HCC from perilesional negative or pseudo- lesions.

In conclusion, in our study, we demonstrated that complementary dynamic and diffusion MRI achieve effective monitoring of tumour response to therapy. DW MR imaging is a rapid promising technique for the noninvasive assessment of tumor response after TACE particularly when contrast medium administration is contraindicated or in patients who could not hold their breath adequately.

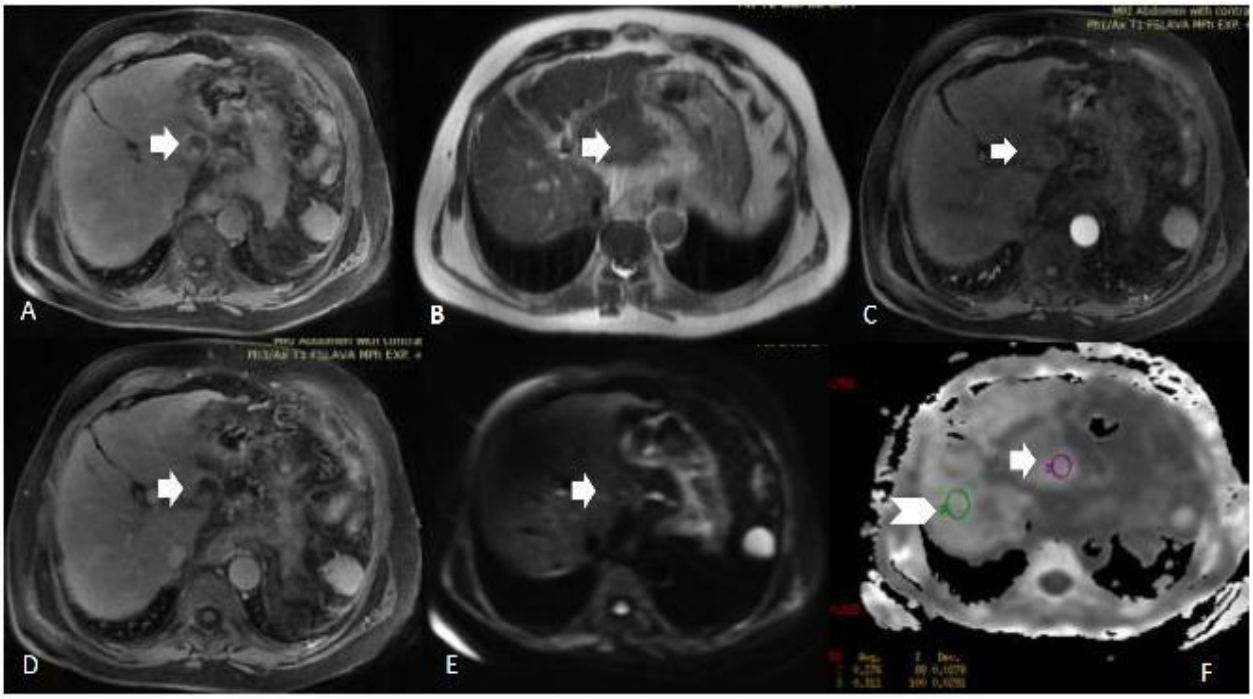

Figure (8): Figure (9): Axial MRI images at the level of the embolized lesions A)T1 weighted image showed heterogeneous predominantly low signal intensity. B) T2 weighted image showed low signal intensity of the lesion. C and D) Dynamic MRI arterial phase and equilibrium phase both showed no evidence of contrast uptake. E) DWI at b value 20 showed no evidence of diffusion restriction. F) ADC value showed high DC value ((measuring about 2.9 x 10^{-3}) arrow compared to the normal liver parenchyma measuring about (2.7 x 10^{-3}) arrow head.

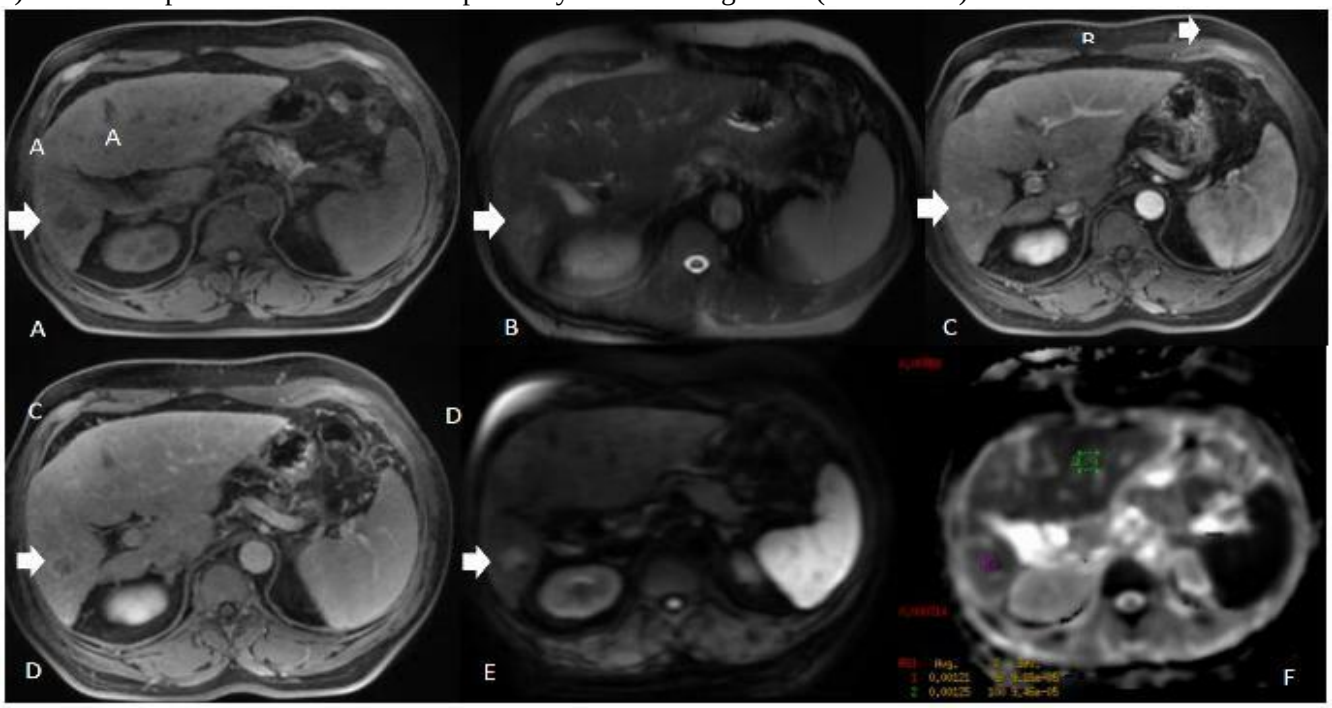

Figure (10): A) Axial MRI T1 weighted image at the level of the right hepatic lobe segment VII lesion showed low signal intensity (arrow). B) Axial MRI T2 weighted image at the level of the right hepatic lobe focal lesion revealed high signal intensity (arrow). C and D) Axial Dynamic) phase 2 (Portovenous phase) and Phase 4 (delayed phase) showed rapid contrast uptake and rapid wash out (mainly nodular uptake) of the right hepatic lobe segment VII lesion denoting residual HCC activity. E MRI Diffusion image at the level of segment VII lesion at b value 500, both showed bright signal intensity denoting diffusion restriction and residual tumor activity. F) ADC value of the same patient revealed average value 1.2 x 10^{-3} (denoting active HCC).

REFERENCES

1. **Mezale D, Strumfa I, Vanags A *et al.* (2017):** Non-alcoholic steatohepatitis, liver cirrhosis and hepatocellular carcinoma: The molecular pathways. In: Tsoulfas G, editor. Liver Cirrhosis – Update and Current Challenges. Rijeka Intech Open, 6: 1-34.
2. **Ali R, Gagan KS (2014):** Hepatocellular carcinoma review: Current treatment, and evidence-based medicine. World J Gastroenterol., 20 (15): 4115–4127.
3. **Özkavukcu E, Haliloğlu N, Erden A (2009):** Post-treatment MRI findings of hepatocellular carcinoma. Diagn Interv Radiol., 15: 111–120.
4. **Lim HS, Jeong YY, Kang HK *et al.* (2006):** Imaging Features of Hepatocellular Carcinoma After Transcatheter Arterial Chemoembolization and Radiofrequency Ablation. AJR., 187: 341–349.
5. **Vossen JA, Buijs M, Kamel IR (2006):** Assessment of tumor response on MR imaging after locoregional therapy. Tech Vasc Interv Radiol., 9: 125–132.
6. **Ippolito D, Grazioli S, Drago G *et al.* (2018):** Recent advances in non-invasive magnetic resonance imaging assessment of hepatocellular carcinoma: World Journal of Gastroenterol., 24 (23): 2413–2426.
7. **Chilla GS, Tan CH, Xu C *et al.* (2015):** Diffusion weighted magnetic resonance imaging and its recent trend a survey. Quant Imaging Med Surg., 5 (3): 407–422.
8. **Kele PG, van der Jagt EJ (2010):** Diffusion weighted imaging in the liver. World J Gastroenterol., 16 (13): 1567-1576.
9. **Guimaraes MD, Hochhegger B, Benveniste MF *et al.* (2014):** Improving CT-guided transthoracic biopsy of mediastinal lesions by diffusion-weighted magnetic resonance imaging. Journal, 69:787-791.
10. **Schraml C, Kaufmann S, Rempp H *et al.* (2015):** Imaging of HCC – Current state of the art. Diagnostics, 5 (4): 513-545.
11. **Brown DB, Cardella JF, Sacks D *et al.* (2006):** Quality improvement guidelines for transhepatic arterial chemoembolization, embolization, and chemotherapeutic infusion for hepatic malignancy. J Vasc Interv Radiol., 17: 225–232.
12. **Rita YWC, Wan WY, Roshni P *et al.* (2016):** Abdominal Imaging Hepatocellular Carcinoma Post Embolotherapy: Imaging Appearances and Pitfalls on Computed Tomography and Magnetic Resonance Imaging Canadian Association of Radiologists Journal, 67: 58-172
13. **Lencioni R, Llovet JM (2010):** Modified RECIST (mRECIST) assessment for hepatocellular carcinoma. Semin Liver Dis., 30: 52e60.
14. **Afifi AH, Naguib AM, Seragaldin F (2016):** Magnetic resonance imaging in assessment of hepatocellular carcinoma after chemoembolization. The Egyptian Journal of Radiology and Nuclear Medicine, 47 (1): 61-71.
15. **Yu J, Kim J, Chung J *et al.* (2009):** Added Value of Diffusion-Weighted Imaging in the MRI Assessment of Perilesional Tumor Recurrence after Chemoembolization of Hepatocellular Carcinomas. Journal OF Magnetic Resonance Imaging, 30: 153–160.
16. **Braga L, Armao D, Azzazi ME *et al.* (2010):** Liver, In Abdominal–Pelvic MRI, 3rd edn. Semelka RC (ed). Wiley-Blackwell: Hoboken, NJ., Pp: 45–454.
17. **Kamel I, Liapi E, Reyes D *et al.* (2009):** Unresectable Hepatocellular Carcinoma: Serial Early Vascular and Cellular Changes after Transarterial Chemoembolization as Detected with MR Imaging. Radiology, 250 (2): 466-73
18. **Kamel I, Bluemke D, Eng J *et al.* (2006):** The Role of Functional MR Imaging in the Assessment of Tumor Response after Chemoembolization in Patients with Hepatocellular Carcinoma. J Vasc Interv Radiol., 17: 505–512
19. **Kamel I, Bluemke D, Ramsey D *et al.* (2003):** Role of Diffusion-Weighted Imaging in Estimating Tumor Necrosis after Chemoembolization of Hepatocellular Carcinoma. AJR., 181 (3): 708-10.
20. **Lee C, Kim KA, Park CM *et al.* (2011):** Hepatic tumor response evaluation by magnetic resonance imaging. Doi:30 10.1594/ecr2011/C-1465.
21. **Kim KW, Lee JM, Choi BI *et al.* (2010):** Assessment of the treatment response of HCC. Abdom Imaging, 36: 300–314.
22. **Goshima S, Kanematsu M, Kondo H *et al.* (2008):** Diffusion-weighted imaging of the liver: optimizing b value for the detection and characterization of benign and malignant hepatic lesions. J Magn Reson Imaging, 28 (3): 691-7.
23. **Liapi E, Geschwind JF, Vossen JA *et al.* (2008):** Functional MRI Evaluation of Tumor Response in Patients with Neuroendocrine Hepatic Metastasis Treated with Transcatheter Arterial Chemoembolization. AJR., 190: 67–73.
24. **Ebeed A, Romeih M, Refat M *et al.* (2017):** Role of dynamic contrast-enhanced and diffusion weighted MRI in evaluation of hepatocellular carcinoma after chemoembolization. The Egyptian Journal of Radiology and Nuclear Medicine, 48: 807-815.
25. **Sahin H, Harman M, Cinar C *et al.* (2012):** Evaluation of treatment response of chemoembolization in hepatocellular carcinoma with diffusion-weighted imaging on 3.0-T MR imaging. Journal of Vascular Interventional Radiology, 23 (2): 241-7.
26. **Koh DM, Collins DJ (2007):** Diffusion-weighted MRI in the body: applications and challenges in oncology. AJR Am J Roentgenol., 188: 1622–1635.
27. **Kandpal H, Sharma R, Madhusudhan KS *et al.* (2009):** Respiratory-triggered versus breath-hold diffusion-weighted MRI of liver lesions: comparison of image quality and apparent diffusion coefficient values. AJR., 192: 915–922
28. **Batra A, Tripathi RP (2004):** Atypical diffusion-weighted magnetic resonance findings in glioblastoma multiforme. Australas Radiol., 48: 388–91.
29. **Jiang Z, Peng W, Li W *et al.* (2008):** Effect of b value on monitoring therapeutic response by diffusion-weighted imaging. World J Gastroenterol., 14 (38): 5893-5899.
30. **Taouli B, Koh DM (2010):** Diffusion-weighted MR imaging of the liver. Radiology, 254: 47- 66.
31. **Chiu FY, Jao JC, Chen CY *et al.* (2005):** Effect of intravenous gadolinium-DTPA on diffusion-weighted magnetic resonance images for evaluation of focal hepatic lesions. J Comput Assist Tomogr., 29 (2): 176-80.
32. **Lin G, Ng KK, Chang CJ *et al.* (2009):** Myometrial invasion in endometrial cancer: diagnostic accuracy of diffusion-weighted 3.0-T MR imaging–initial experience. Radiology, 250: 784–792.
33. **Thoeny HC, De Keyzer F, Chen F *et al.* (2005):** Diffusion-weighted MR imaging in monitoring the effect of a vascular targeting agent on rhabdomyosarcoma in rats. Radiology, 234: 756–764.